In-depth NMR and IR study of the proton transfer equilibrium between $[\{(MeC(CH_2PPh_2)_3\}Ru(CO)H_2]$ and hexafluoroisopropanol

Vladimir I. Bakhmutov, Ekaterina V. Bakhmutova, Natalia V. Belkova, Claudio Bianchini, Lina M. Epstein, Dante Masi, Maurizio Peruzzini, Elena S. Shubina, Evgenii V. Vorontsov, and Fabrizio Zanobini

Abstract: The (carbonyl)dihydride complex $[(triphos)Ru(CO)H_2]$ (**2**) has been synthesized by reaction of the ruthenate $[(triphos)RuH_3]K$ (triphos = $MeC(CH_2PPh_2)_3$) with ethanol saturated with CO. A single crystal X-ray analysis and IR and NMR experiments have shown that **2** adopts in both the solid state and solution an octahedral coordination geometry with a *facial* triphos ligand, two *cis* terminal hydrides, and a terminal carbonyl. The reaction of hexafluoro-2-propanol (HFIP) with **2** has been studied in CH_2Cl_2 solution by IR and NMR spectroscopy. The proton donor interacts with a terminal hydride of **2** forming a rather strong hydrogen bond. The resulting H-bonded adduct $[\{(triphos)Ru(CO)(H)H\}\cdots\{HOCH(CF_3)_2\}]$ (**2a**) has fully been characterized by in situ NMR and IR techniques. Compound **2a** is in equilibrium with the nonclassical η^2-H_2 complex $[(triphos)Ru(CO)H(H_2)]^+$ (**2b**), which can independently be prepared by protonation of **2** with a strong protic acid at low temperature. Unequivocal characterization of the dihydrogen complex (**2b**) has been achieved by a multifaceted spectroscopic investigation ($T_{1\min}^{obs}$ = 0.005 s (200 MHz), $J_{H,D} \approx 30$ Hz, DQCC = 78.3 kHz). A combined IR and NMR study of the proton transfer reaction involving **2** and HFIP in CH_2Cl_2 to give, first, the H-bonded adduct (**2a**) and, then, the dihydrogen complex (**2b**) has demonstrated that all these species are in equilibrium in the temperature range from 190 to 260 K. The thermodynamic parameters for the formation of **2a** have independently been determined by NMR and IR methods, while those for the formation of **2b** have been obtained by IR spectroscopy. An energetic profile for the reaction sequence **2** $\rightarrow$ **2a** $\rightarrow$ **2b** is proposed and discussed.

Key words: hydrides, hydrogen bonding, ruthenium, IR spectroscopy, NMR spectroscopy.

Résumé : On a synthétisé le complexe $[(triphos)Ru(CO)H_2]$ (**2**) (triphos = $MeC(CH_2PPh_2)_3$), un (carbonyl)dihydrure, en faisant réagir le ruthénate $[(triphos)RuH_3]K$ avec de l'éthanol saturé de CO. La diffraction des rayons X sur un cristal unique et des expériences d'IR et de RMN ont permis de montrer que le composé **2**, tant à l'état solide qu'en solution, adopte une géométrie de coordination octaédrique comportant un ligand triphos *facial*, deux hydrures terminaux *cis* et un carbonyle terminal. Faisant appel à la spectroscopie IR et RMN, on a étudié la réaction du composé **2** avec l'hexafluoropropan-2-ol (HFIP) en solution dans le CH_2Cl_2. Le donneur de proton interagit avec un hydrure terminal du composé **2** en formant une liaison hydrogène relativement forte. Faisant appel in situ d'IR et de RMN, on a fait un caractérisation complète de l'adduit à liaison hydrogène qui en résulte $[\{(triphos)Ru(CO)(H)H\}\cdots\{HOCH(CF_3)_2\}]$ (**2a**). Le composé **2a** est en équilibre avec le complexe non classique η^2-H_2, $[(triphos)Ru(CO)(H_2)]^+$ (**2b**) que l'on peut préparer de façon indépendante en procédant à la protonation du composé **2** à l'aide d'un acide protique fort, à basse température. On a effectué la caractérisation non ambiguë du complexe dihydrogéné, **2b**, en faisant appel à une étude spectroscopique à multiples facettes ($T_{1\min}^{obs}$ = 0,005 s (200 MHz), $J_{H,D} \approx 30$ Hz, DQCC = 78,3 kHz). Faisant appel à une combinaison de techniques d'IR et de RMN, on a étudié la réaction de transfert de proton du composé **2** avec l'HFIP, dans le CH_2Cl_2, qui donne premièrement l'adduit à liaison hydrogène **2a** et ensuite le complexe dihydrogéné **2b**; ces études ont démontré que toutes ces espèces sont en équilibre sur toute la plage de températures allant de

---

Received August 30, 2000. Published on the NRC Research Press Web site at http://canjchem.nrc.ca on May 23, 2001.

Dedicated to Professor Brian James on the occasion of his 65th birthday in recognition of his outstanding work in organometallic chemistry and homogeneous catalysis.

V.I. Bakhmutov,[1,2] E.V. Bakhmutova,[1] N.V. Belkova, L.M. Epstein,[1,2] E.S. Shubina, and E.V. Vorontsov. A.N. Nesmeyanov Institute of Organoelement Compounds, Vavilov str. 28, V-334, Moscow, Russia, 117813.
C. Bianchini,[2] D. Masi, M. Peruzzini, F. Zanobini. Istituto per lo Studio della Stereochimica ed Energetica dei Composti di Coordinazione, ISSECC-CNR, Via Jacopo Nardi, 39, 50132, Firenze, Italy.

[1] Present Address: Centro de Investigación y de Estudios Avanzados del I.P.N., Apdo postal 14–740, 07000, México D.F., México.

[2] Corresponding authors (fax: 39-055-247-8366; e-mail: bianchini@fi.cnr.it; vladimir@mail.cinvestav.mx; epst@ineos.ac.ru; peruz@fi.cnr.it).

DOI: 10.1139/cjc-79-5/6-479

190–260 K. Faisant appel à l'IR et à la RMN, on a déterminé de façon indépendante les paramètres thermodynamiques pour la formation du composé **2a** alors que ceux pour la formation de **2b** ont été obtenus par spectroscopie IR. On propose et on discute d'un profil énergétique pour la séquence des réactions **2** → **2a** → **2b**.

Mots clés : hydrures, liaison hydrogène, ruthénium, spectroscopie IR, spectroscopie RMN.

[Traduit par la Rédaction]

Introduction

The occurrence of intra- and intermolecular hydrogen bonds between transition-metal hydride complexes and Brønsted acids has recently been established for a variety of metals and proton donors (1). It is proposed that such M-H···H-X interactions in solution may lead to the formation of dihydrogen (η^2-H_2) complexes; however, well-documented examples of proton transfers involving the formation of η^2-H_2 metal complexes via M-H···H-X intermediates are still very scarce (2). This scarcity of data is essentially due to the low temperature at which the M-H···H-X $\leftrightarrows$ $M(H_2)^+$ + X^- equilibrium becomes spectroscopically visible (2*b*, *d*, *f*). Nonetheless, the energetic profile associated with the M-H + ROH $\leftrightarrows$ M-H···HOR $\leftrightarrows$ $M(H_2)^+$ + RO^- sequence relative to the reaction of the rhenium(I) complex [(triphos)Re$(CO)_2$H] (triphos = MeC$(CH_2PPh_2)_3$) (**1**) with perfluoro-*tert*-butanol has recently been estimated using a combined NMR–IR approach (2*e*). In particular, the H-bonded adduct [(triphos)Re$(CO)_2$H···HOR] (**1a**) was unambiguously intercepted by in situ IR and NMR experiments before degradation to the thermodynamically stable dihydrogen complex [(triphos)Re$(CO)_2(\eta^2$-$H_2)]^+$ (**1b**) (2*b*). The energy associated with each step of the conversion of **1a** to **1b** was determined, and a neat energy profile for the whole proton transfer process was obtained (2e). Prior to the rhenium study, thermodynamic parameters relative to the (M-H + HOR $\leftrightarrows$ M-H···HOR)→ M-(η^2-H_2) step had been reported exclusively for the reaction of the dihydride *trans*-[RuH_2(dppm)$_2$] (dppm = bis-diphenylphosphinomethane) with phenol in toluene (2*a*).

This paper is aimed at expanding our knowledge on proton-transfer reactions involving transition metal hydrides, as well as showing the reliability and wide applicability of the combined NMR–IR approach to study M-H + ROH $\leftrightarrows$ M-H···HOR $\leftrightarrows$ $M(H_2)^+$ + RO^- solution equilibria. To this purpose, the new dihydride complex [(triphos)Ru(CO)H_2] (**2**) has been synthesized, and the energetic profile associated with the formation of the hydrogen-bonded adduct [{(triphos)Ru(CO)(H)H}···{HOCH$(CF_3)_2$}] (**2a**) and of the dihydrogen complex [(triphos)Ru(CO)H$(H_2)]^+$ (**2b**) has been determined by means of low-temperature NMR and IR experiments.

Experimental

General procedures

Tetrahydrofuran (THF) was purified by distillation under nitrogen over $LiAlH_4$. All other reagents and chemicals were reagent grade and, unless otherwise stated, were used as received by commercial suppliers. All reactions and manipulations were routinely performed under a dry nitrogen atmosphere by using standard Schlenk-tube techniques. The solid complexes were collected on sintered glass-frits and washed with ethanol and light petroleum ether (bp 40–60°C) before being dried with a stream of nitrogen. The complex [(triphos)RuH(η^2-BH_4)] (**3**) was prepared as described in the literature (3).

NMR studies were carried out in standard 5-mm-NMR tubes in either CD_2Cl_2 or THF-d_8. The deuterated solvents were dried by using conventional procedures and were freshly distilled under inert atmosphere prior to use. ^{1}H and ^{2}H NMR spectra were recorded on Bruker AC200, WP-200 or AMX-400 spectrometers and were calibrated with respect to tetramethylsilane. ^{31}P NMR spectra were recorded on the Bruker AC200 instrument operating at 81.01 MHz. Chemical shifts were measured relative to external 85% H_3PO_4 with downfield values taken as positive. ^{13}C NMR spectra were recorded on Varian VXR 300 or Bruker AC200 spectrometers operating at 75.42 or 50.32 MHz, respectively. Peak positions are relative to tetramethylsilane and were calibrated against the residual solvent resonance. The conventional inversion-recovery method (180-τ-90) was used to determine the variable-temperature longitudinal-relaxation time (T_1). The relaxation times were calculated using the nonlinear three-parameter fitting routine of the spectrometers. In each experiment, the waiting period was five times larger than the expected relaxation time and 16–20 variable delays were employed. The duration of the pulses were controlled at every temperature. The errors in T_1 determinations were lower than 5% (this was checked with different samples). The proton donor-hydride reactions were carried out in cold (195–250 K) CD_2Cl_2 solutions in 5-mm-NMR tubes and all the NMR experiments were run starting at low temperature with precooled probe-heads.

Infrared spectra were recorded as Nujol™ mulls on a PerkinElmer 1600 series FT-IR spectrometer between KBr plates or in CH_2Cl_2 solutions on a Specord M82 spectrometer using 0.01–0.2 cm CaF_2 cells. The latter measurements were performed under a dry argon atmosphere. Low-temperature IR measurements were carried out in CH_2Cl_2 solutions using a Carl Zeiss Jena cryostat. The accuracy of the experimental temperature was ±0.5 K. The cells width was 0.04–0.12 cm.

Elemental analyses (C, H) were performed at ISSECC CNR using a Carlo Erba model 1106 elemental analyzer.

Preparation of [(triphos)Ru(CO)H_2] (2)

A vigorously stirred suspension of [(triphos)RuH(η^2-BH_4)] (**3**) (600 mg, 0.81 mmol) in THF (30 mL) was treated with solid KO-*t*-Bu (270 mg, 2.41 mmol) added in small portions. After 30 min stirring, the starting pale yellow complex dissolved to yield a colorless solution which was layered with absolute ethanol (20 mL) saturated with carbon monoxide (CO). After 15 min, the CO flow was stopped and a brisk stream of nitrogen was passed throughout the solution until ivory colored crystals of **2** separated. Yield: 415 mg (78%). Slow crystallization of the mother liquor in the air gave a second crop of **2** (80 mg, 15%). Ivory-colored truncated prisms of **2** suitable for an X-ray crystal analysis were obtained by slow evaporation of the solvent from a diluted CH_2Cl_2–EtOH solution (2:1 v/v). IR (KBr, Nujol™) (cm^{-1}): 1920 (CO), 1884 (RuH), 1859; (CH_2Cl_2 solution) 1934 (CO), 1871 (RuH). $^{31}P\{H\}$ NMR (22°C, CD_2Cl_2, 81.01 MHz) δ: 34.71 (AM_2 spin system, t, $^2J_{P_A,P_M}$ = 32.9 Hz, P_A), 27.07 (d, $^2J_{P_M,P_A}$ = 32.9 Hz, P_M). ^1H NMR (22°C, CD_2Cl_2, 200.13 MHz) δ: 7.8–6.9 (m, 30H, aromatic protons), 2.4–2.1 (m, 6H, $CH_{2(triphos)}$), –1.48 (q, $^4J_{H,P}$ = 2.9 Hz, 3H, $CH_{3(triphos)}$), –7.32 (AA′XX′Y, $^2J_{H_A,H_{A'}}$ = 6.0 Hz, $^2J_{H_A,P_X}$ = 18.2 Hz, $^2J_{H_A,P_{X'}}$ = 66.1 Hz, $^2J_{H_A,P_Y}$ = 18.0 Hz, $^2J_{P_X,P_{X'}}$ = 38.0 Hz, 2H, RuH). $^{13}C\{H\}$ NMR (22°C, CD_2Cl_2, 50.32 MHz) δ: 209.98 (dt, $^2J_{C,P_{trans}}$ = 77.5 Hz, $^2J_{C,P_{cis}}$ = 7.8 Hz, CO), 142, 138 (m, aromatic ipso carbons), 134–128 (m, aromatic *meta*, *ortho*, and *para* carbons), 39.36 (q, $^3J_{C,P}$ = 9.4 Hz, CH_3), 39.11 (q, $^2J_{C,P}$ = 7.0 Hz, CCH_3), 35.71 (td, $J = J_{C,P_{equat}} + J_{C,P'_{equat}}$ = 12.5 Hz, $J_{C,P_{axial}}$ = 4.7 Hz, CH_2P_{equat}), 33.98 (dt, $J_{C,P_{axial}}$ = 20.3 Hz, $J_{C,P_{equat}}$ = 6.2 Hz, CH_2P_{axial}). Anal. calcd. for $C_{42}H_{41}OP_3Ru$: C 66.8, H 5.5; found C 66.4, H 5.6.

Preparation of [(triphos)Ru(CO)D_2] (**2-*d*$_2$**)

The perdeuterated isotopomer [(triphos)Ru(CO)D_2] (**2b-*d*$_2$**) was prepared as described above using [(triphos)RuD(η^2-BD_4)] (**3-*d*$_4$**) in the place of **3** and C_2H_5OD instead of ethanol. IR (KBr) (cm^{-1}): 1349 (m) (RuD). ^1H NMR analysis confirmed an isotopic purity higher than 95%.

Preparation of [(triphos)Ru(CO)H(H_2)]$^+$ (2b)

A 5-mm screw-cap NMR tube was charged with **2** (40 mg, 5.3×10^{-2} mmol) and degassed dichloromethane-d_2 (0.8 mL). Into this solution, cooled to –78°C with a dry ice–acetone bath, was added via syringe an excess of $HBF_4\cdot OMe_2$ (20 μL, 0.16 mmol). The tube was immediately inserted into the spectrometer precooled at –80°C and a $^{31}P\{H\}$ NMR spectrum, immediately recorded at this temperature, revealed the quantitative transformation of **2** into **2b**. $^{31}P\{H\}$ NMR (–80°C, CD_2Cl_2, 81.01 MHz) δ: 20.19 (AM_2 spin system, t, $^2J_{P_M,P_A}$ = 35.3 Hz, P_A), 22.90 (d, $^2J_{P_A,P_M}$ = 35.3 Hz, P_M). ^1H NMR (–80°C, CD_2Cl_2, 200.13 MHz) δ: 7.7–7.0 (m, 30H, aromatic protons), 2.7–2.1 (m, 6H, $CH_{2(triphos)}$), 1.58 (br, 3H, $CH_{3(triphos)}$), –5.39 (br, 3H, RuH).

Monitoring the reaction between 2 and HFIP

*Interception of the hydrogen-adduct [{(triphos)Ru(CO)(H)H}···{HOCH(CF_3)$_2$}] (**2a**)*

Under similar experimental conditions, two equiv of HFIP (11.2 μL, 0.11 mmol) were added via syringe to a solution of **2** prepared as described above. Low temperature NMR spectra showed the complete conversion of **2** into the hydrogen-adduct **2a**. $^{31}P\{H\}$ NMR (–80°C, CD_2Cl_2, 81.01 MHz) δ: 30.95 (AM_2 spin system, t, $^2J_{P_M,P_A}$ = 34.5 Hz, P_A), 24.47 (d, $^2J_{P_A,P_M}$ = 34.5 Hz, P_M). ^1H NMR (–80°C, CD_2Cl_2, 200.13 MHz) δ: 8.1–6.8 (m, 30H, aromatic protons), 2.4–2.0 (m, 6H, $CH_{2(triphos)}$), 1.43 (br, 3H, $CH_{3(triphos)}$), –7.79 (br, 2H, RuH).

*Transformation of the hydrogen-adduct into [(triphos)Ru(CO)H(H_2)]$^+$ (**2b**)*

Addition of a large excess of HFIP (12 equiv, 67 μL) to the above solution at –80°C immediately transformed the hydrogen-adduct **2a** into the molecular hydrogen complex **2b**. ^{31}P NMR spectroscopy showed that the transformation of **2a** in **2b** occurred in almost quantitative yield. Complex **2b** was also obtained by addition 10–12 equiv of HFIP to a dichloromethane-d_2 solution of **2** (NMR tube experiment carried out at –80°C).

Preparation of [(triphos)Ru(CO)$_2$H](BPh_4) (5)

A solution of **2** (250 mg, 0.33 mmol) in THF (15 mL) was saturated with CO and then 1 equiv of MeOTf (40 μL, 0.36 mmol) was added via syringe under stirring. After 15 min, CO was replaced by nitrogen, and $NaBPh_4$ (300 mg, 0.88 mmol) in ethanol (15 mL) was added. Slow concentration of the resulting colorless solution gave off-white crystals of **5** in ca. 95% yield. The IR and NMR characteristics of **5** are fully coincident with those reported in the literature for the same compound prepared by a different route (4).

X-ray diffraction study of [(triphos)Ru(CO)H_2] (2)

An ivory-colored crystal of **2** with the dimensions 0.22 × 0.12 × 0.17 mm was chosen for an X-ray analysis. A summary of crystal and intensity data for the compound is presented in Table 1. Experimental data were recorded at room temp on a PHILIPS PW1100-FEBO diffractometer using a graphite-monochromated Cu Kα radiation. A set of 25 carefully centered reflections in the range $10° \le \theta \le 15°$ was used for determining the lattice constants. As a general procedure, the intensity of three standard reflections was measured periodically every 2 h for orientation and intensity control. This procedure did not reveal any decay of intensities. The data were corrected for Lorentz and polarization effects. Atomic scattering factors were those tabulated by Cromer and Waber (5) with anomalous dispersion corrections taken from ref 6. An empirical absorption correction was applied via Ψ scan with transmission factors in the range 1.8794–1.0042. The computational work was performed with a Pentium-II™ personal computer using the programs SHELXL 93 (7) and ZORTEP (8). Final atomic coordinates with equivalent isotropic thermal parameters of all atoms and structure factors are available as supplementary material.

The structure was solved via the heavy atom technique using the program SIR 92 (9) and all the non-hydrogen atoms were found through a series of F_0 Fourier maps. Refinement was done by full-matrix least-squares calculations, initially with isotropic thermal parameters, and then, in the last least-squares cycle, with anisotropic thermal parameters for ruthenium, phosphorus, and carbon and oxygen atoms of the carbonyl ligand. All of the phenyl rings were treated as rigid bodies with D_{6h} symmetry and C—C distances fixed at 1.39 Å. Hydrogen atoms of the triphos ligand were introduced in calculated positions, but not refined. At an advanced stage of the refinement, two hydrogen atoms were located in the Fourier map and successfully refined as ruthenium coordinated hydrides.

Results and discussion

Synthesis and characterization of the dihydride complex [(triphos)Ru(CO)H_2] (2)

Treatment of the known (tetrahydroborate)hydride complex [(triphos)RuH(η^2-BH_4)] (**3**) with a slight excess of KO-*t*-Bu in anhydrous THF at room temp gave a yellow-orange solution of the trihydride [(triphos)RuH_3]K (**4**) as the only Ru-containing product (Scheme 1) (10). Although **4** can be

Table 1. Crystal data and structure refinement for **2**.

Empirical formula	$C_{42}H_{41}OP_3Ru$
Formula weight	755.78
Temperature (K)	293(2)
Wavelength (Å)	1.54180
Crystal system	Orthorombic
Space group	$P21/b$
Unit cell dimensions	a = 16.886(6) Å
	α = 90.00(2)°
	b = 20.845(9) Å
	β = 90.00(2)°
	c = 10.2770(10) Å
	γ = 90.00(2)°
Volume (Å^3)	3617(2)
Z	4
Density (calcd.) (Mg m^{-3})	1.388
Absorption coefficient (mm^{-1})	5.003
$F(000)$	1560
Crystal size (mm)	0.22 × 0.12 × 0.17
Theta range for data collection (°)	4.24–50.02
Index ranges	$-2 \leq h \leq 16$; $0 \leq k \leq 20$; $-2 \leq l \leq 10$
Reflections collected	1832
Independent reflections	1831 ($R(int)$ = 0.0374)
Refinement method	Full-matrix least-squares on F^2
Data/restraints/parameters	1831/1/158
GoF on F^2	1.074
Final R indices [$I > 2\sigma(I)$]	$R_1 = 0.0796$, $wR_2 = 0.2039$
R indices (all data)	$R_1 = 0.0836$, $wR_2 = 0.2107$
Absolute structure parameter	–0.03(3)
Largest diff. peak and hole (e Å^{-3})	1.286 and –1.400

isolated as potassium salt in the presence of a 18-crown-6 ether, its difficult storage, due to remarkable sensitivity to water and protic solvents, makes freshly prepared THF solutions excellent vehicles to study the chemistry of the ruthenate **4** and, in particular, to generate the 16e$^-$ fragment [(triphos)Ru(H)$_2$]. As a matter of fact, a THF solution of **4** reacts with protic solvents such as water or alcohols to give quantitatively the tetrahydrido complex [{(triphos)RuH}$_2$(μ-H)$_2$] and H_2 via spontaneous dimerization of the coordinatively unsaturated fragment [(triphos)RuH$_2$].[3] In the presence of σ-donor ligands, this 16e$^-$ system can be intercepted to form stable octahedral complexes of the formula [(triphos)Ru(L)H$_2$] (L = nitriles, phosphines, arsines, CO, etc.).[3] With carbon monoxide, the new carbonyl dihydride complex [(triphos)Ru(CO)H$_2$] (**2**) was readily obtained by simply adding ethanol saturated with CO to a THF solution of **4**. Once formed, **2** is stable in THF and can be isolated in the solid state. Compound **2** is air-stable in both the solid state and solution (THF, halocarbons, acetone) and has been characterized by multinuclear (^{1}H, ^{31}P, and ^{13}C) NMR and IR spectroscopy, and elemental and X-ray diffraction analyses (vide infra).

The AM$_2$ pattern featured in the ^{31}P NMR spectrum of **2** and the typical AA′XX′Y (X, X′, Y = ^{31}P) pattern of the high-field hydride resonance (δ = –7.32) are consistent with the presence of two *cis*-disposed hydride ligands in an octahedral coordination with three positions taken by a *facial* (*fac*) triphos and three other positions occupied by two hydrides and one carbon monoxide ligand (11). A narrow doublet of triplets is contained in the ^{13}C NMR spectrum at δ 209.98 for the CO carbon atom, which agrees with the proposed structural formulation for **2**.

Complex **2** is stereochemically rigid on the NMR time scale; neither the ^{31}P nor the ^{1}H NMR spectrum show significant changes over the temperature window of dichloromethane. In keeping with a classical dihydride nature, a variable-temperature analysis of the spin-lattice relaxation time (T_1) of the isochronous hydride ligands gave a quite long minimum value of 0.178 s at 200 K using a 200 MHz instrument (12). The solid state IR spectrum contains a ν(CO) band at 1920 cm^{-1} and two ν(RuH) bands at 1884 and 1859 cm^{-1}. The observation of a medium intensity absorption at ca. 1350 cm^{-1} in the spectrum of the deuterated isotopomer **2b-*d*$_2$** confirmed the correctness of our ν(RuH) assignment ($k_{H/D}$ = 1.39). The IR spectrum in CH_2Cl_2 solution shows ν(CO) at 1934 cm^{-1} and ν(RuH) at 1871 cm^{-1}. This latter band is a combination of both ν_s(RuH) and ν_{as}(RuH), which are well-resolved in the solid state (ν_s(RuH) 1884 cm^{-1} and ν_{as}(RuH) 1859 cm^{-1}).

Well-shaped crystals of **2** were grown from a dilute dichloromethane–ethanol solution. Figure 1 shows a ORTEP view of the complex molecule, while crystallographic data and selected bond distances and angles are presented in Tables 1 and 2, respectively. The results of a single crystal

---

[3] C. Bianchini and M. Peruzzini, unpublished results.

Scheme. 1.

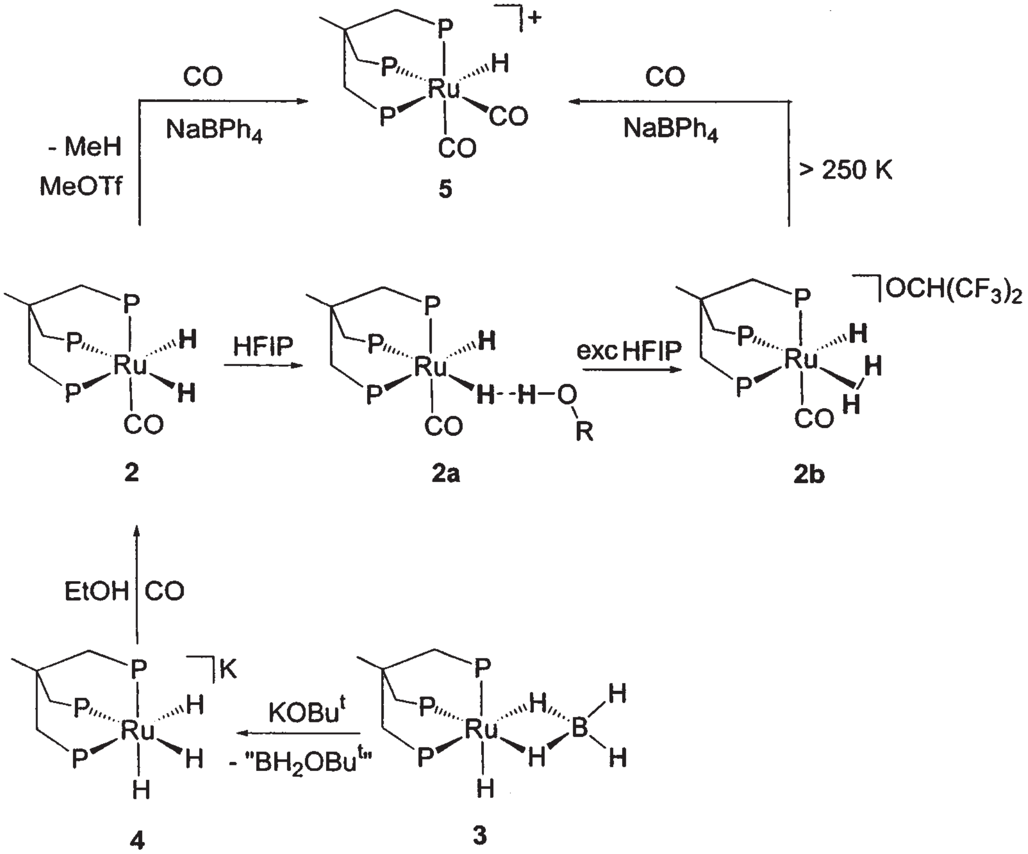

Fig. 1. ORTEP drawing of the molecular structure of **2**. Only the ipso carbons of the six triphos phenyl rings are shown.

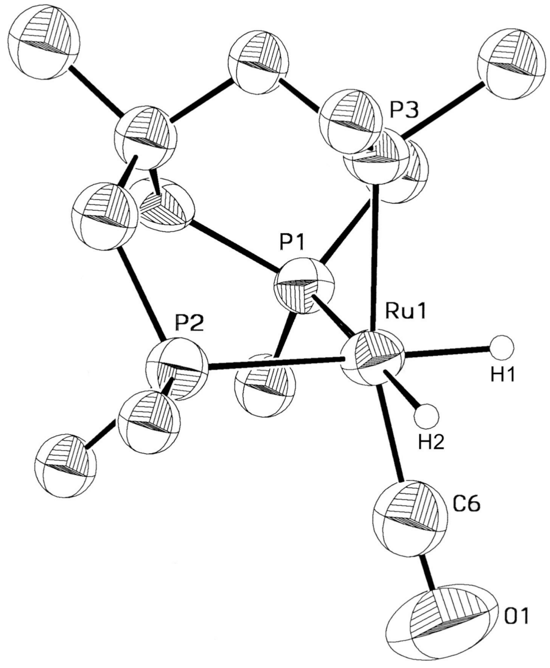

X-ray diffraction analysis are consistent with the solution structure determined by NMR spectroscopy.

The ruthenium atom is octahedrally coordinated by a *fac* triphos ligand, by two *cis* hydrides, and by a terminal carbonyl. The observed distortions from a regular octahedron are typical of triphos complexes containing hydride ligands (13). The three Ru—P distances are very similar to each other (average Ru—P = 2.34 Å), and reflect comparable *trans* influence exerted by the hydride and the carbonyl ligands. The Ru—CO distance of 1.84(2) Å is typical for ruthenium(II) carbonyl complexes (14). The two hydride ligands were located in the difference Fourier maps and refined as isotropic atoms together with the rest of the non-hydrogen atoms of the structure, giving Ru—H(1) and Ru—H(2) separations of 1.46(18) and 1.50(11) Å, respectively.

Synthesis and spectroscopic characterization of the dihydrogen complex $[(triphos)Ru(CO)(H)(H_2)]^+$ (2b)

Treatment of **2** with strong protic acids (HBF_4, $HOSO_2CF_3$) at room temp gave a mixture of products that denied first-order analysis, thus indicating that the molecular hydrogen complex $[(triphos)Ru(CO)(H)(H_2)]^+$ (**2b**), which actually forms upon protonation of **2** (vide infra), is unstable at room temp. This behavior agrees with the results by Michos et al. (15) for the protonation of $[\{PhP(CH_2CH_2PPh_2)_2\}RuH_2L]$ (L = CO, $P(OCH_2)_3CEt$, PMe_2Ph), which did not afford isolable molecular hydrogen complexes, although the spectroscopic data were provided. However, when the protonation was repeated in the presence of carbon monoxide, the known octahedral hydrido dicarbonyl complex $[(triphos)Ru(CO)_2H]^+$ was quantitatively produced and isolated as the tetraphenylborate salt $[(triphos)Ru(CO)_2H](BPh_4)$ (**5**). Complex **5** has previously been synthesized by oxidation of the ruthenium(0) complex

Table 2. Selected bond lengths and angles for **2**.

Bond lengths (Å)	
Ru(1)—C(6)	1.84(2)
Ru(1)—P(1)	2.334(5)
Ru(1)—P(2)	2.340(5)
Ru(1)—P(3)	2.344(5)
Ru(1)—H(1)	1.46(18)
Ru(1)—H(2)	1.50(11)
O(1)—C(6)	1.20(3)
P(1)—C(1)	1.873(19)
P(2)—C(2)	1.881(19)
P(3)—C(3)	1.856(18)
C(1)—C(4)	1.56(2)
C(2)—C(4)	1.50(3)
C(3)—C(4)	1.57(2)
C(4)—C(5)	1.58(3)
Bond angles (°)	
C(6)-Ru(1)-P(1)	107.4(7)
C(6)-Ru(1)-P(2)	101.9(7)
P(1)-Ru(1)-P(2)	89.54(17)
C(6)-Ru(1)-P(3)	162.1(8)
P(1)-Ru(1)-P(3)	87.17(18)
P(2)-Ru(1)-P(3)	88.19(17)
C(6)-Ru(1)-H(1)	81(8)
P(1)-Ru(1)-H(1)	110(7)
P(2)-Ru(1)-H(1)	158(7)
P(3)-Ru(1)-H(1)	84(8)
C(6)-Ru(1)-H(2)	65(4)
P(1)-Ru(1)-H(2)	172(4)
P(2)-Ru(1)-H(2)	96(4)
P(3)-Ru(1)-H(2)	99(4)
H(1)-Ru(1)-H(2)	66(8)
O(1)-C(6)-Ru(1)	176(2)

[(triphos)Ru(CO)$_2$] with HCl or MeCOCl (4). To intercept the molecular hydrogen complex **2b**, the protonation of **2** was then carried out in CH_2Cl_2 solution at low-temperature (200 K) using either a stoichiometric amount of strong acid or a large excess (10–12 equiv) of a medium-strength proton donor such as the activated alcohol hexafluoroisopropanol (HFIP). Indeed, the addition of 12 equiv of HFIP to a CD_2Cl_2 solution of **2** in a 5 mm NMR tube cooled to 195 K generated a new broad hydride resonance centered at ca. –5.4 ppm (3H) featured by a very short $T_{1\text{min}}$ value of 0.005 s at 190 K (200 MHz), which is typical for a nonclassical dihydrogen structure (16, 17). The appearance of the η^2-H_2 resonance in the proton spectrum of **2b** was paralleled by that of a well-resolved AMM′ pattern with δ_{P_A} 20.19 and δ_{P_M} 22.90 ppm (J_{P_A,P_M} = 35.3 Hz) in the ^{31}P NMR spectrum. The P_A donor atom, *trans* to the CO ligand, undergoes a significant high-field shift ($\Delta\delta \approx 14.5$ ppm) in line with the formation of a cationic carbonyl complex. Figure 2 collects the NMR spectra illustrating the stepwise transformation of **2** into **2b** via the H-bonded adduct [{(triphos)Ru(CO)(H)H}···{HOCH(CF$_3$)$_2$}] (**2a**). Indeed, this latter compound is formed in very low concentration when a large excess of HFIP is employed (Fig. 2*c*), while it is the only product visible on the ^{31}P NMR timescale when **2** is reacted with two equiv of alcohol (vide infra).

Fig. 2. ^{31}P NMR spectra (81.01 MHz) illustrating the stepwise transformation of **2** (4.63 × 10^{-5} M solution in CD_2Cl_2) (top trace), into **2a** (middle trace) upon addition of HFIP (2 equiv) and, eventually, into **2b** (bottom trace) upon addition of further 10 equiv of HFIP. All the spectra were taken at 193 K.

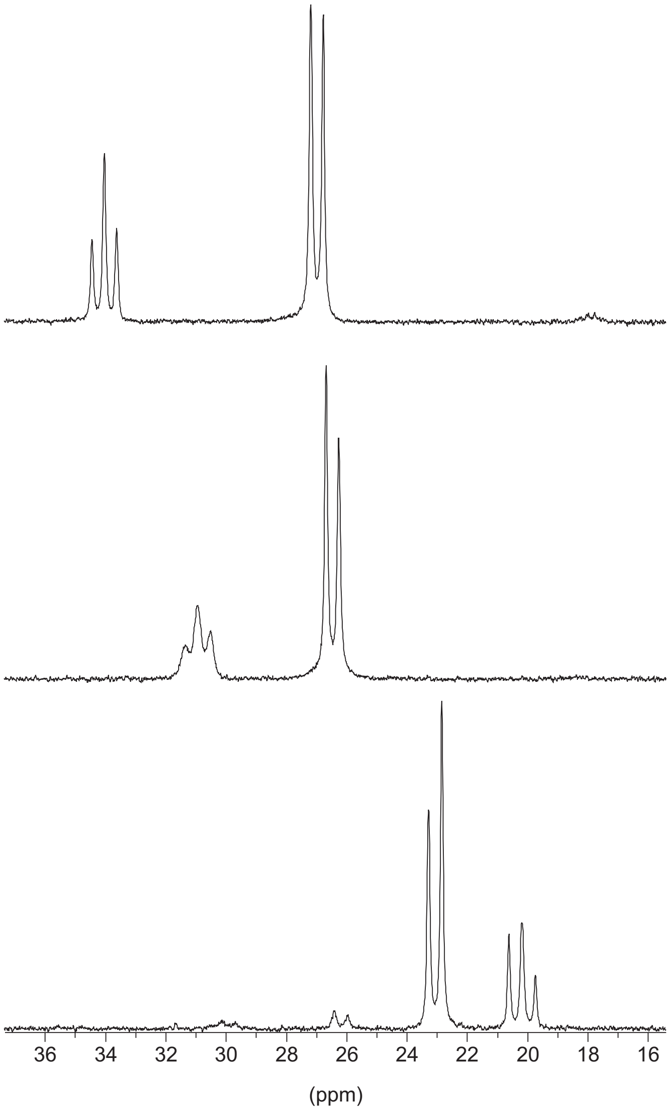

The dihydrogen complex **2b** is highly fluxional in CD_2Cl_2 solution as a consequence of a fast hydride-dihydrogen exchange occurring even at the lowest temperature investigated (180 K). Compound **2b** is quite stable in solution below 250 K but slowly eliminates H_2 above this temperature as shown by the appearance of the typical H_2 resonance at 4.56 ppm in the proton NMR spectrum. The decomposition of **2b** is not chemoselective; in fact, a single, well-defined product was obtained only in the presence of external ligands, like carbon monoxide, which are capable of trapping the 16e$^-$ fragment [(triphos)Ru(CO)H]$^+$.

The nonclassical nature of **2b** was confirmed by deuterium labeling experiments. A ^{1}H{^{31}P} NMR spectrum, recorded after addition of excess CF_3COOD to a solution of **2** in CD_2Cl_2 at 200 K, exhibits a poorly resolved resonance at –5.48 ppm, which, upon increasing the temperature to 250 K, transforms into a nonbinomial quintet with a line separation of ca. 10 Hz. Accordingly, this resonance can

Fig. 3. Hydride region of the $^1H\{^{31}P\}$ NMR spectrum of the $\mathbf{2}$-$\boldsymbol{d_2}$ isotopomer (250 K, 400 MHz) prepared by low-temperature protonation of **2** with an excess of CF_3COOD in CD_2Cl_2.

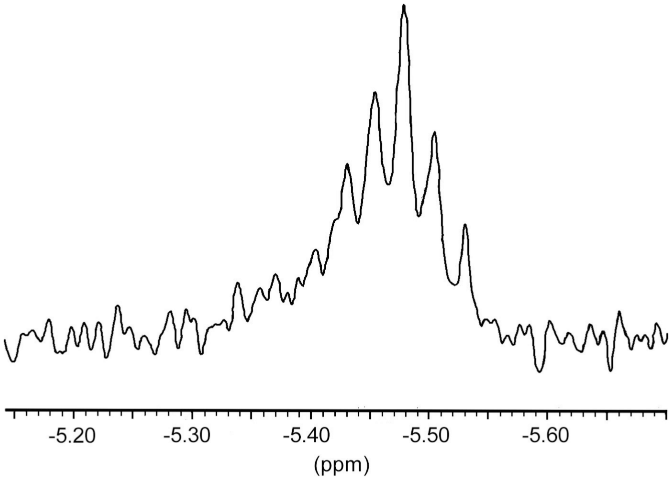

safely be assigned to the bis-deuterated isotopomer $[(\mathrm{triphos})Ru(CO)HD_2]^+$ ($\mathbf{2b}$-$\boldsymbol{d_2}$) (Fig. 3). In the ^1H NMR spectrum, the typical 1:1:1 triplet of free HD is also observed at 4.51 ppm. In agreement with the formation of a deuterated isotopomer of **2b**, the deuteration results in a high-field isotopic shift of the "HD_2" signal of 120 ppb. Similar isotopic shifts are commonly observed for HD metal complexes (17) and may be due to the IPR effect. A $J_{\mathrm{H,D}}$ constant of ca. 30 Hz can be calculated for **2b** assuming a very fast H–H_2 exchange (17). Introducing this value in the empirical correlation, $r_{(\mathrm{HH})} = (1.42 - 0.0167)J_{\mathrm{H,D}}$ Å, recently proposed by Morris and co-workers (18) for dihydrogen complexes, a rather elongated H—H distance of 0.92 Å may be figured out for the nonclassical ligand in **2b**.

An independent estimation of the H—H separation can also be obtained from the relaxation data. The $T_{1\mathrm{min}}$ measured for both the hydride signals in **2** ($T_{1\mathrm{min}}$ ($\mathbf{2}_{\mathrm{Ru,H2}}$) = 0.178 s) and **2b** ($T^{\mathrm{obs}}_{1\mathrm{min}}$ ($\mathbf{2b}_{\mathrm{Ru,H3}}$) = 0.005 s) allows one to calculate the $T_{1\mathrm{min}}$ for the dihydrogen ligand in **2b** by means of eq. [1], and hence the $T_{1\mathrm{min}}$ (Ru(H_2)) applying eq. [2].

$$[1] \qquad 1/T^{\mathrm{obs}}_{1\mathrm{min}}(\mathbf{2b}_{\mathrm{Ru,H3}}) = (1/3)/T_{1\mathrm{min}}\,(\mathbf{2}_{\mathrm{Ru,H2}}) + (2/3)/T^{\mathrm{obs}}_{1\mathrm{min}}(\mathbf{2b}_{\mathrm{Ru(H2)}})$$

$$[2] \qquad 1/T^{\mathrm{obs}}_{1\mathrm{min}}\,(\mathbf{2b}_{\mathrm{Ru(H2)}}) = 1/T_{1\mathrm{min}}\,(\mathbf{2}_{\mathrm{Ru,H2}}) + 1/T_{1\mathrm{min}}\,(\mathbf{2b}_{\mathrm{Ru(H2)}})$$

As a result, a $T_{1\mathrm{min}}$ ($\mathbf{2b}_{\mathrm{Ru(H2)}}$) value of 0.0035 s, exclusively occasioned by hydride–hydride dipole–dipole interactions in the dihydrogen ligand, is obtained, which ultimately gives an H—H distance ranging from 0.74 to 0.94 Å depending on the spinning model adopted (fast or slow rotation) for the motion of the dihydrogen ligand (19*a*). As the separation of 0.94 Å calculated using the low-spinning model is very close to the distance determined from the $J_{\mathrm{H,D}}$ coupling constant in $\mathbf{2b}$-$\boldsymbol{d_2}$, it is conceivable that **2b** contains, as usually, a rather "immobile" H_2 ligand (19*b*).

Since the relaxation properties of the deuterium nucleus are a powerful tool to investigate the dynamic behavior of dihydrogen ligands (16*b*, 21), ^2H-T_1 spin-lattice measurements were carried out on complexes $\mathbf{2b}$-$\boldsymbol{d_2}$ and $\mathbf{2b}$-$\boldsymbol{d_3}$ in CH_2Cl_2. The perdeuterated isotopomer $\mathbf{2b}$-$\boldsymbol{d_3}$ has been prepared by low-temperature protonation of $\mathbf{2b}$-$\boldsymbol{d_2}$ with CF_3COOD. The ^2H NMR spectrum of $\mathbf{2b}$-$\boldsymbol{d_3}$ contains a broad resonance at ca. –5.4 ppm that can safely be assigned to the three freely exchanging deuterides. Like **2b**, the ^2H resonance of $\mathbf{2b}$-$\boldsymbol{d_3}$ remains unchanged even at 180 K due to fast deuteride–deuterium exchange.

The ^2H-T_1 relaxation experiments on the parent classical deuteride $\mathbf{2b}$-$\boldsymbol{d_2}$ give a $T_{1\mathrm{min}}$ ($\mathbf{2}_{\mathrm{Ru,D2}}$) value of 0.0149 s at 61.402 MHz. By applying eq. [3] and introducing therein $\eta = 0$ (21), a deuterium quadrupole coupling constant (DQCC) (22) as large as 78.3 kHz can be calculated for $\mathbf{2b}$-$\boldsymbol{d_2}$

$$[3] \qquad \mathrm{DQCC} = 1.2201(1 + \eta^2/3)^{-1/2}\,(\nu/T_{1\mathrm{min}})^{1/2}$$

where DQCC, ν, and $T_{1\mathrm{min}}$ are given in kHz, MHz, and s, respectively.

The DQCC value for $\mathbf{2}$-$\boldsymbol{d_2}$ is very close to those recently determined for classical deuteride ligands in the related complexes $[(\mathrm{dppe})_2RuD(D_2)]BPh_4$ (dppe = $PPh_2CH_2CH_2PPh_2$) (DQCC = 79 kHz) (20*b*) and $[(PP_3)RuD_2]$ (PP_3 = $P(CH_2CH_2PPh_2)_3$) (DQCC = 73–76 kHz) (20*a*). The average ^2H resonance in $\mathbf{2b}$-$\boldsymbol{d_3}$ exhibits a $T_{1\mathrm{min}}$ ($\mathbf{2b}_{\mathrm{Ru,D3}}$) time of 0.0174 s. Taking into account a fast D–D_2 exchange (see eq. [1]), it is then possible to calculate a $T_{1\mathrm{min}}$ value of 0.0190 s for the nonclassical D_2 ligand in $\mathbf{2b}$-$\boldsymbol{d_3}$. Nonclassical transition metal hydride complexes have been reported to display longer ^2H-$T_{1\mathrm{min}}$ times as compared to classical polyhydrides due to motions of the dihydrogen ligands (20). The elongation observed on going from $\mathbf{2b}$-$\boldsymbol{d_2}$ to $\mathbf{2b}$-$\boldsymbol{d_3}$, however, is very weak, which may be due to a slow-rotating dihydrogen ligand. Thus, the evaluation of ^2H-$T_{1\mathrm{min}}$ (or DQCC) is important because it provides an additional support for the genuine nonclassical nature of **2b**.

The IR spectrum of the dihydrogen complex **2b**, obtained by treatment of **2** with HBF_4 at 200 K in dichloromethane solution, shows a ν(CO) band at 2023 cm^{-1}, which is shifted at higher energy as compared to the ν(CO) band of the initial complex. Such high-frequency shifts are commonly observed for transformations of hydride(carbonyl) complexes into cationic nonclassical molecular hydrogen-carbonyl derivatives (2*b*, *f*).

Synthesis and spectroscopic characterization of the H-bonded adduct $[\{(\mathrm{triphos})Ru(CO)(H)H\}\cdots\{HOCH(CF_3)_2\}]$ (2a)

Upon addition of **2** (0.07 M) to a CH_2Cl_2 solution of trifluoroethanol (TFE), HFIP, MeOH, or monofluoroethanol (MFE) at 298 K, significant changes were observed in the ν_{OH} region of the corresponding IR spectrum. To avoid self-association, proton-donor concentrations in the range 0.01–0.03 M were used, so as to work with an excess of **2**. Irrespective of the proton donor, the changes affecting the OH stretching region (Table 3) were indicative of a hydrogen bonding interaction between the alcohol and the hydride ligands in the ruthenium complex.[4] Indeed, the intensity of the

---

[4] A hydrogen-bonding interaction between the activated alcohol and the oxygen atom of the carbonyl ligand was ruled out in view of the high-frequency shift encompassed by ν_{CO} upon addition of HFIP (1*d*, 2*b*).

Table 3. Spectral characteristics of the H-bonded adducts [{(triphos)Ru(CO)(H)H}⋯{HOR}] and enthalpy values (–ΔH) relative to their formation in CH_2Cl_2.

ROH	ν_{OH}^{bonded} (cm^{-1})	$\Delta\nu_{OH}$ (cm^{-1})	$-\Delta H$ (kcal mol^{-1})	E_j
CH_3OH	3415	212	4.1	1.41
MFE	3355	254	4.7	1.38
TFE	3254	346	5.8	1.40
HFIP	3160	420	6.6	1.37

band due to the free OH groups decreased, while a new broad and intense band was formed at lower frequency. As previously observed (1*d*, 2*f*), the frequency shifts ($\Delta\nu = \nu_{OH}^{free} - \nu_{OH}^{bonded}$) increase with the proton-donor ability of the alcohol in the order MeOH < MFE < TFE < HFIP.

The Iogansen correlation shown in eq. [4] may be used to estimate the hydrogen-bonding enthalpy values at 298 K from the experimental frequency shifts listed in Table 3 (1*d*, 2*b*).

$$[4] \qquad -\Delta H^\circ = 18\ \Delta\nu/(720 + \Delta\nu)$$

On decreasing the temperature, the band shift ($\Delta\nu_{CO}$) gradually moved to high-frequency reaching a maximum of +15 cm^{-1} at 190 K for a 10-fold excess of alcohol, while a band shift to low-frequency was displayed by the Ru—H stretching of **2**. Indeed, after addition of HFIP (2 to 3 equiv) and cooling down the solution, the ν_{RuH} band at 1871 cm^{-1} moved to low-frequency by 20 cm^{-1}, which is consistent with a hydrogen bonding interaction between the alcohol and a hydride ligand of **2** (1*d*, 2*f*). This behavior led us to assign the two bands at 1949 (ν_{CO}) and 1851 (ν_{RuH}) cm^{-1} to the H-bonded complex **2a**. In contrast, when both the parent hydride **2** and the H-bonded adduct **2a** were contemporaneously present in solution, a unique ν_{CO} and ν_{RuH} band was observed in a position intermediate between the two limits and depending on the molar fraction of **2a** (p(**2a**)). This latter can readily be calculated from eq. [5]

$$[5] \qquad p(\mathbf{2a}) = \frac{\nu_{CO}(\mathbf{2} + \mathbf{2a}) - \nu_{CO}(\mathbf{2})}{\nu_{CO}(\mathbf{2a}) - \nu_{CO}(\mathbf{2})}$$

Using the p(**2a**) data obtained in this way, the formation constants $K_{\mathbf{2-2a}}$ = [**2a**]/[**2**][HFIP] have been determined in the temperature range from 200 to 260 K, and hence the enthalpy and entropy values associated with the formation of **2a** have been calculated by the van't Hoff method. The corresponding temperature dependence of ln $K_{\mathbf{2-2a}}$ vs. $1/T$ shown in Fig. 4 gave a $-\Delta H^\circ_{\mathbf{2a}}$ value of 6.7 kcal mol^{-1} in fairly good agreement with the value calculated from eq. [4]. A $-\Delta S^\circ_{\mathbf{2a}}$ value of 19.6 eu was similarly determined from the plot.

Following the method reported by Iogansen (23), the basicity factor (E_j) of the hydride ligand in **2** was calculated as 1.39 ± 0.02 (1*d*, 2*b*). It is worth noticing that this parameter, which characterizes the absolute proton accepting ability of the hydride ligand, irrespective of both proton donor partner and solvent, is significantly greater than those reported for rhenium hydride **1** (E_j = 0.97) and other metal hydride complexes (2*b*) as well as organic bases such as Et_2O (E_j = 1.0) and DMSO (E_j = 1.27) (23). The relatively high E_j value of **2** might explain why this dihydride complex is easily protonated to give the dihydrogen complex **2b** even with relatively weak proton donors such as HFIP and PFTB.

Fig. 4. Temperature-dependence of the equilibrium constant ($K_{\mathbf{2-2a}}$) for the formation of **2a** from **2** and HFIP in CH_2Cl_2 (obtained from IR data).

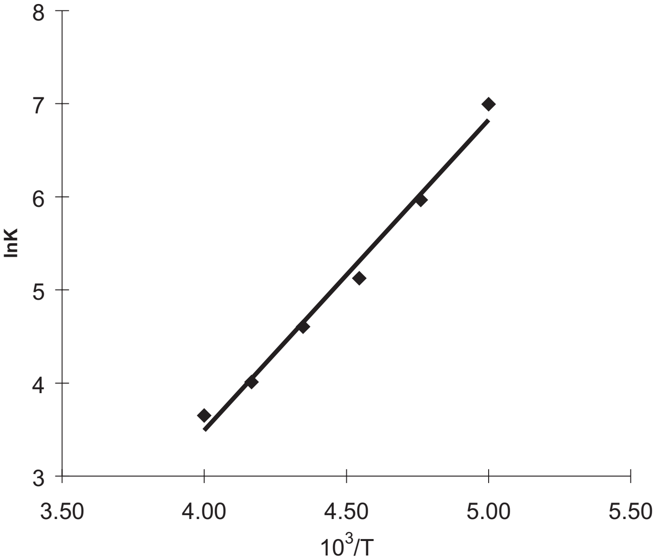

Fig. 5. Variable-temperature IR spectra (ν_{CO} range) of complex **2** (0.006 M) in CH_2Cl_2 at 190 K (curve 1) and in the presence of a 10-fold excess of HFIP in the temperature range between 230 and 190 K (curves 2–6).

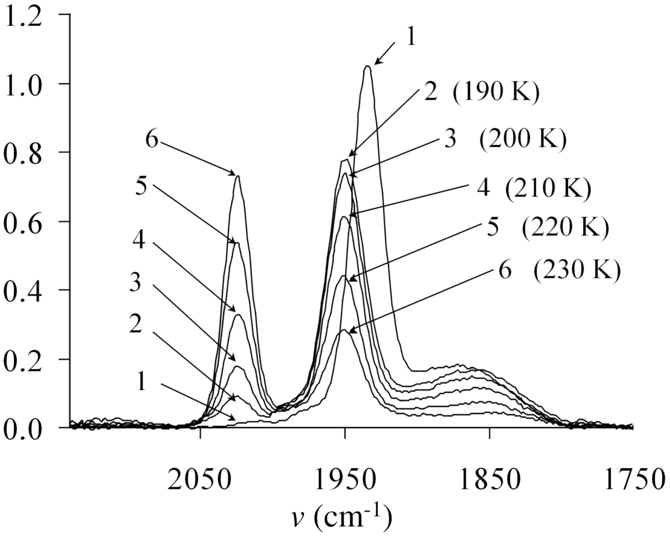

Variable-temperature IR and NMR studies of the proton transfer reactions between 2 and HFIP

The reaction of **2** with HFIP (10–12 equiv) was followed by IR spectroscopy in CH_2Cl_2 starting from 200 K. Selected variable-temperature spectra in the ν_{CO} region are reported in Fig. 5. The spectrum at 200 K showed the presence of the dihydrogen complex **2b**, with ν_{CO} at 2023 cm^{-1}, and of the H-bonded adduct **2a** with ν_{CO} at 1949 cm^{-1}. When the temperature was increased to 260 K, the ν_{CO} band of **2b** decreased in intensity while that of **2a** increased.

Table 4. Temperature-dependence of the equilibrium constants between **2**, **2a**, and **2b** in the presence of HFIP determined from the variable-temperature ^{1}H NMR and IR spectra (range 200–240 K).

T (K)	$K_{\mathbf{2-2a}}$ (mol^{-1})^a	$K_{\mathbf{2a-2b}}$^{b}	$K_{\mathbf{2-2b}}$ (mol^{-1})^b
200	4.6×10^3	2.9×10^3	2.7×10^0
210	1.8×10^3	3.4×10^3	8.6×10^{-1}
215	1.0×10^3		
220	8.3×10^2	4.9×10^1	2.9×10^{-1}
225	5.2×10^2		
230	3.7×10^2	1.6×10^1	1.6×10^{-1}
240	2.6×10^2		

[a] Determined from NMR data.
[b] Determined from IR data.

Concomitantly, an enhancement of the ν_{RuH} band due to **2a** at ca. 1855–1860 cm^{-1} was observed.

Since the equilibrium between **2a** and **2b** is reversible in the temperature range from 200 to 260 K, the IR spectra allowed us to determine the equilibrium constants $K_{\mathbf{2a-2b}} = [\mathbf{2b}]/[\mathbf{2a}]$ and the overall constant $K_{\mathbf{2-2b}} = [\mathbf{2b}]/[\mathbf{2}][\mathrm{HFIP}]$ for the proton transfer from HFIP to a terminal hydride of **2** to give the dihydrogen complex **2b** via the intermediate H-bonded complex **2a**.

The equilibrium concentrations [**2b**] were obtained directly from the IR experiments. The equilibrium concentrations [**2**], [**2a**], [**2b**], and [HFIP] are related to each other and to the total concentration of hydride (c_2) and proton donor (c_{HFIP}) by the mass-balance eqs. [6*a*] and [6*b*].

$$[6a] \qquad c_2 = [\mathbf{2}] + [\mathbf{2a}] + [\mathbf{2b}]$$

$$[6b] \qquad c_{HFIP} = [\mathrm{HFIP}] + [\mathbf{2a}] + [\mathbf{2b}]$$

Substituting for [**2**] and [HFIP] from eqs. [6*a*] and [6*b*] into equation for $K_{\mathbf{2-2a}}$ and rearranging, eq. [7] was obtained whose solution gave [**2a**].

$$[7] \qquad [\mathbf{2a}]^2 + [\mathbf{2a}]\left\{2[\mathbf{2b}] - c_2 - c_{HFIP} - \frac{1}{K_{\mathbf{2-2a}}}\right\} + \{c_2 c_{HFIP} + [\mathbf{2b}]^2 - [\mathbf{2b}](c_2 + c_{HFIP})\} = 0$$

Once the concentrations of each species participating in the proton transfer equilibrium were known, the calculation of the equilibrium constants $K_{\mathbf{2a-2b}}$ and $K_{\mathbf{2-2b}}$ in the temperature range from 200 to 230 K was straightforward (Table 4).

The temperature dependencies of the equilibrium constants with inverse temperature (1/*T*) are linear and provide the following thermodynamic parameters: $-\Delta H^\circ_{\mathbf{2a-2b}}$ = 8.7 kcal mol^{-1}, $-\Delta S^\circ_{\mathbf{2a-2b}}$ = 42 eu for the formation of **2b** from **2a** and $-\Delta H^\circ_{\mathbf{2-2b}}$ = 16.1 kcal mol^{-1}, $-\Delta S^\circ_{\mathbf{2-2b}}$ = 65 eu for the overall proton transfer. Since the formation of **2a** has been found to involve a $-\Delta H^\circ_{\mathbf{2-2a}}$ value of 6.7 kcal mol^{-1}, it is apparent that the formation of **2a** plays the major role in the proton transfer reaction.

The proton transfer reaction for the system (**2** + HFIP) has also been studied by NMR spectroscopy. The low-temperature addition (200 K) of a twofold excess of HFIP to a CH_2Cl_2 solution of **2** results in a high-field shift of the hydride resonance to –7.86 ppm. Figure 6 illustrates the temperature dependence of the hydride chemical shift observed for this solution. The hydride chemical shift of **2** is practically independent from the temperature in the absence of the proton donor (curve 1), while it reaches a plateau at –7.87 ppm below 200 K (curve 2). Therefore, the resonance at –7.87 ppm can be assigned to the H-bonded adduct **2a**. Obviously, the observed hydride resonance is averaged between two nonequivalent positions and, therefore, the chemical shift of the hydride involved in hydrogen bonding can be calculated as –8.29 ppm by eq. [8].

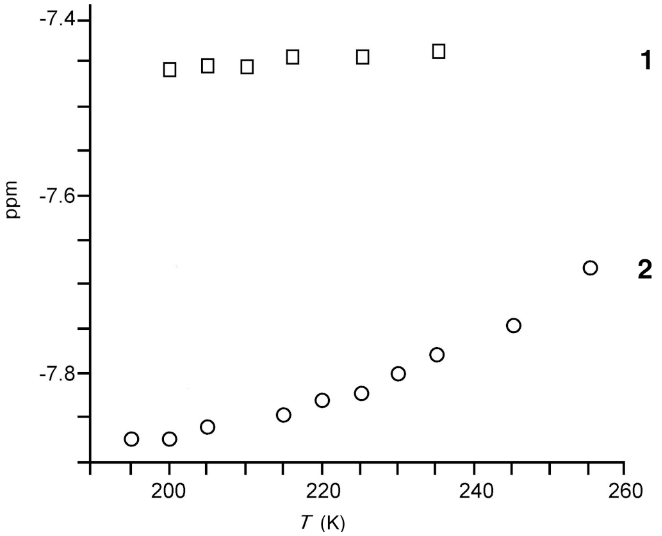

Fig. 6. Temperature-dependence of the chemical shift of the hydride resonance of **2** in CD_2Cl_2 (□), and in the presence of a twofold excess of HFIP (○).

$$[8] \qquad \delta(\mathrm{RuH})^{\mathrm{obs}} = 0.5\ \delta(\mathrm{RuH}^{\mathrm{free}}) + 0.5\ \delta(\mathrm{RuH}\cdots\mathrm{HOR})$$

From curve 2 in Fig. 6, the molar fractions of **2** (p_{free}) and **2a** (p_{bonded}) were obtained at different temperatures (eq. [9]) and the corresponding equilibrium constants for the formation of the H-bonded complex could be calculated (Table 4). Finally, the $-\Delta H^\circ$ (7.1 kcal mol^{-1}) and $-\Delta S^\circ$ (19.0 eu) values relative to the formation of **2a** were obtained from a standard ln *K* vs. 1/*T* plot.

$$[9] \qquad \delta(\mathrm{RuH})^{\mathrm{obs}} = p_{\mathrm{free}}\ \delta(\mathrm{RuH}^{\mathrm{free}}) + p_{\mathrm{bonded}}\ \delta(\mathrm{RuH}^{\mathrm{bonded}})$$

It is worth noticing that the thermodynamic parameters calculated using variable-temperature NMR and IR experiments are in good agreement with each other.

Positive enthalpy and entropy changes (ΔH° = 17 kcal mol^{-1}, ΔS° = 75.8 eu) obtained by NMR methods have been reported for the proton transfer from phenol to the hydride ligand in $[\mathrm{RuH_2(dppm)_2}]$ (2*a*), while the thermodynamic parameters for the proton transfer to $[\mathrm{RuH_2(dmpe)_2}]$ (dmpe = bis(dimethylphosphino)ethane) in ethanol (the H-bonded complex was not observed, however) exhibit a negative sign and are only slightly smaller than ours ($-\Delta H^\circ$= 6.0 kcal mol^{-1}, $-\Delta S^\circ$ = 19.9 eu) (24).

It is also worth noticing that the H-bonded complex (**2a**) is thermodynamically more stable than corresponding rhenium complex (**1a**) ($-\Delta H^\circ$ = 4.8 kcal mol^{-1}) (2*b*), which

Scheme 2.

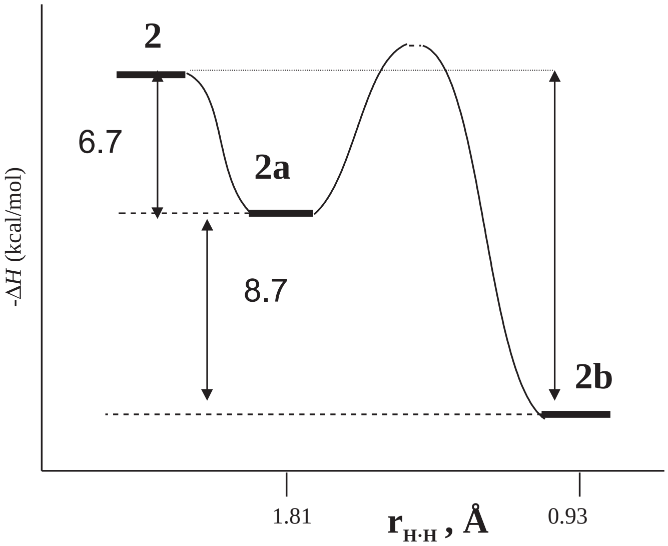

reflects the lower basicity of the hydride ligand in **1** (see the E_j factor).

The variable-temperature spin-lattice relaxation data for a CH_2Cl_2 solution of **2** in the presence of a twofold excess of HFIP showed that the relaxation time of the observed hydride resonance reaches a minimum at 200 K ($T_{1\min}^{\mathrm{obs}}$ = 0.119 s at 200 MHz). As it is evident from Fig. 5, under these conditions the equilibrium is completely shifted towards the formation of **2a**. Using eq. [10], the observed $T_{1\min}^{\mathrm{obs}}$ value was employed to calculate $T_{1\min}^{\mathrm{obs}}$ (RuH···HFIP) (0.0894 s) for the H-bonded hydride ligand in **2a**. Finally, the combination of $T_{1\min}^{\mathrm{obs}}$ (RuH···HFIP) and of T_1 (0.178 s) measured for **2** (see above) provided a $T_{1\min}$ (H···H) value of 0.183 s for **2a**, which is exclusively due to hydride–proton dipole–dipole interactions (12).

$$[10] \qquad 1/T_{1\min}^{\mathrm{obs}} = 0.5/0.178 + 0.5/T_{1\min}^{\mathrm{obs}}\ (\mathrm{RuH\cdots H})$$

Using the procedure described by Halpern and co-workers (12), the $T_{1\min}$ (H···H) relaxation time has been employed to calculate a hydride—proton distance of 1.81 Å in **2a**, which is quite comparable to the value reported for the rhenium system (**1** + PFTB) (1.83 Å) (2*b*). This H—H distance lies in the expected range (1.7–2.0 Å) for transition metal hydride complexes with either intra- (1*a*–*c*) or intermolecular hydrogen bonds (1*d*, *e*).

We have already shown that **2** (0.008 M) is converted to **2b** in the presence of a 12-fold excess of HFIP in CD_2Cl_2. The dihydrogen complex is clearly observed in the ^1H NMR spectrum at 183 K (see above), which also contains an averaged hydride resonance for **2** and **2a**. Consistent with the IR data, it has been found that increasing the temperature leads to a completely reversible redistribution of integral intensities of both signals, thus indicating that all these species are in equilibrium.

An energetic profile for the overall hydrogen-transfer reaction is illustrated in Scheme 2. It is worth noticing that: (*i*) the hydride—proton distance represents the reaction coordinate (determined by NMR spectroscopy); (*ii*) the energy of **2a** is obtained by IR and NMR data; (*iii*) the depth of the second well corresponds to the enthalpy value obtained from the IR data; and (*iv*) the energy level of the transition state for the proton transfer **2a** → **2b** has a purely qualitative character.

Notwithstanding the qualitative character of the profile, the proposed energy levels are quite reasonable. Indeed, it is well known that the formation of H-bonded adducts is a diffusion-controlled process with no energy barrier (25). The observation of separated signals for the hydride ligands in **2a** and **2b**, with no broadening of the resonances at low-temperature, is consistent with a lifetime longer than 10 s for this reaction (26). Accordingly, an upper limit of 10^{-1} s^{-1} can be envisaged for the corresponding rate constant. The bottom limit of rate constant may roughly be estimated considering that our IR technique does not allow one to monitor band-intensity changes for processes faster than 1×10^{-2} s^{-1} (2*e*). Since no intensity change with time is observed, it may be assumed that the lifetime of the proton transfer is shorter than 1 to 2 min, which provides a lower limit of 1×10^{-2} s^{-1} for the rate constant. It may be thus concluded that the transformation of **2a** into **2b** has an activation barrier $-\Delta G^{\ddagger}$ (200 K) of ca. 12 to 13 kcal mol^{-1}, which is in nice agreement with the barrier previously calculated for the related rhenium system [(triphos)Re$(CO)_2$H] with PFTB (2*e*) as well as other literature data. In particular, theoretical studies of proton transfer to Re- and Ru-hydrides have recently shown that the proton-transfer barriers depend on both the metal complex basicity and the strength of the acid and may vary from 10 to 0.7 kcal mol^{-1} (27). On the other hand, rather low rates of proton transfer and dihydrogen complex generation (varying from 1×10^6 to 1×10^{-1} s^{-1} with corresponding activation barriers of ca. 6.5–12 kcal mol^{-1}) have been reported for the reactions of Fe- and Ru-hydrido complexes with strong acids (28).

Conclusions

The (carbonyl)dihydride complex [(triphos)Ru(CO)H_2] (**2**) has been found to react with hexafluoro-2-propanol to give the new dihydrogen complex [(triphos)Ru(CO)H(H_2)]$^+$ (**2b**) through the H-bonded adduct [{(triphos)Ru(CO)(H)H}···{HOCH$(CF_3)_2$}] (**2a**). All these compounds have been characterized by in situ NMR and IR techniques. Variable-temperature IR and NMR studies in CH_2Cl_2 solution have shown that **2**, **2a**, and **2b** are in equilibrium in the temperature range from 190 to 260 K. An energetic profile describing the formation of the dihydrogen complex via the H-bonded adduct has been proposed on the basis of thermodynamic parameters determined experimentally. The proposed energy profile suggests that, at least in thermodynamic terms, the formation of the H-bonded adduct contributes substantially to the overall proton transfer leading to the dihydrogen complex.

Acknowledgments

Thanks are due to NATO (contract "^{2}H-relaxation as a tool to study hydrogen transfer reactions", grant HTECH-CRG 972 135), CNR (Italy) – RAS (Russian Federation) agreement, and RFBR (project No 99–03–33270) for financial support. Support from COST Chemistry Action D17/WG003 is also acknowledged.

References

1. (*a*) A.J. Lough, S.Park, R. Ramashandrar, and R.H. Morris. J. Am. Chem. Soc. **116**, 8356 (1994); (*b*) J.C. Lee, E. Peris, A. Rheinhold, and R.H. Crabtree. J. Am. Chem. Soc. **116**, 11014 (1994); (*c*) E. Peris, J.C. Lee, J.R. Rambo, O. Eisenstein, and R.H. Crabtree. J. Am. Chem. Soc. **117**, 3485 (1995); (*d*) E.S. Shubina, N.V. Belkova, A.N. Krylov, E.V. Vorontsov, L.M. Epstein, D.G. Gusev, M. Niedermann, and H. Berke. J. Am. Chem. Soc. **118**, 1105 (1996); (*e*) N.V. Belkova, E.S. Shubina, A.V. Ionidis, L.M. Epstein, H. Jacobsen, A. Messmer, and H. Berke. Inorg. Chem. **36**, 1522 (1997).
2. (*a*) J.A. Ayllon, C. Gervaux, S. Sabo-Etienne, and B. Chaudret. Organometallics, **16**, 2000 (1997); (*b*) E.S. Shubina, N.V. Belkova, E.V. Bakhmutova, E.V. Vorontsov, V.I. Bakhmutov, A.V. Ionidis, C. Bianchini, L. Marvelli, M. Peruzzini, and L.M. Epstein. Inorg. Chim. Acta, **280**, 302 (1998); (*c*) Y. Guari, J.A. Aylonn, S. Sabo-Etienne, and B. Chaudret. Inorg. Chem. **37**, 640 (1998); (*d*) S. Grundemann, S. Ulrich, H.H. Limbach, N.S. Golubev, G.S. Denisov, L.M. Epstein, S. Sabo-Etienne, and B. Chaudret. Inorg. Chem. **38**, 2550 (1999); (*e*) N.V. Belkova, E.V. Bakhmutova, E.S. Shubina, C. Bianchini, M. Peruzzini V.I. Bakhmutov and L.M. Epstein. Eur. J. Inorg. Chem. 2163 (2000); (*f*) N.V. Belkova, E.S. Shubina, E.I. Gutsul, L.M. Epstein, I.L. Eremenko, and S.E. Nefedov. J. Organomet. Chem. (2000) in press.
3. L.F. Rhodes and L.M. Venanzi. Inorg. Chem. **26**, 2692 (1987).
4. S.I. Hommeltoft and M.C. Baird. Organometallics, **5**, 190 (1986).
5. D. Cromer and J. Waber. Acta Crystallogr. **18**, 104 (1965).
6. A.J.C. Wilson (*Editor*). International tables for X-ray crystallography. Vol. C. Kluwer Academic Press, Dordrecht. 1992. p. 219
7. G.M. Sheldrick. SHELXL. 93 Program for crystal structure refinement. University of Göttingen, Germany. 1993.
8. C.K. Johnson. Report ORNL-5138. Oak Ridge National Laboratory, Oak Ridge, TN. 1976; as modified by L. Zsolnai and H. Pritzkow. University of Heidelberg, Germany. 1994.
9. A. Altomare, G. Cascarano, G. Giacovazzo, and A. Gualandi. J. Appl. Crystallogr. **26**, 343 (1993).
10. C. Bianchini, A. Meli, S. Moneti, and F. Vizza. Organometallics, **17**, 2636 (1998).
11. (*a*) P. Barbaro, C. Bianchini, A. Meli, M. Peruzzini, and F. Vizza. Organometallics, **10**, 2227 (1991); (*b*) C. Bianchini, S. Moneti, M. Peruzzini, and F. Vizza. Inorg. Chem. **36**, 5818 (1997); (*c*) C. Bianchini, A. Meli, M. Peruzzini, F. Vizza, P. Frediani, and J.A. Ramirez. Organometallics, **9**, 226 (1990).
12. P.J. Desrosiers, L. Cai, Z. Lin, R. Richards, and J. Halpern. J. Am. Chem. Soc. **113**, 4173 (1991).
13. J. Ott, L.M. Venanzi, C.A. Ghilardi, S. Midollini, and A. Orlandini. J. Organomet. Chem. **291**, 89 (1985).
14. A.G. Orpen, L. Brammer, F.H. Allen, O. Kennard, D.G. Watson, and R. Taylor. J. Chem. Soc. Dalton Trans. S1 (1989).
15. D. Michos, X.-L. Luo, and R.H. Crabtree. Inorg. Chem. **31**, 4245 (1992).
16. (*a*) P.G. Jessop and R.H. Morris. Coord. Chem. Rev. **121**, 155 (1992); (*b*) V.I. Bakhmutov and E.V. Vorontsov. Rev. Inorg. Chem. **18**, 183 (1998).
17. W.J. Oldham, A.S. Hinkle, and D.M. Heinekey. J. Am. Chem. Soc. **119**, 11028 (1997).
18. P.A. Maltby, M. Schlaf, M. Steinbeck, A.J. Lough, R.H. Morris, W.T. Klooster, T.F. Koetzle, and R.C. Srivastava. J. Am. Chem. Soc. **118**, 5396 (1996).
19. (*a*) R.H. Morris and R.J. Witterbort. Magn. Reson. Chem. **35**, 243 (1997); (*b*) D.G. Gusev, R.L. Kuhlman, K.B. Renkema, O. Eisenstein, and K.G. Caulton. Inorg. Chem. **35**, 6775 (1996).
20. (*a*) V.I. Bakhmutov, C. Bianchini, F. Maseras, A. Lledos, M. Peruzzini, and E.V. Vorontsov. Chem. Eur. J. **5**, 3318 (1999); (*b*) G.A. Facey, T.P. Fong, D. Gusev, P.M. Macdonald, R.H. Morris, M. Schlaf, and W. Xu. Can. J. Chem. **77**, 1899 (1999); (*c*) V.I. Bakhmutov, C. Bianchini, M. Peruzzini, F. Vizza, and E.V. Vorontsov. Inorg. Chem. **39**, 1655 (2000).
21. D. Nietlispach, V.I. Bakhmutov, and H. Berke. J. Am. Chem. Soc. **115**, 9191 (1993).
22. (*a*) H. Guo, W.L. Jarret, and L.G. Butler. Inorg. Chem. **26**, 3001 (1987); (*b*) L.G. Butler and E.A. Keiter, J. Coord. Chem. **32**, 121 (1992); (*c*) A.J. Kim, F.R. Fronczek, L.G. Butler, S. Chen, and E.A. Keiter. J. Am. Chem. Soc. **113**, 9090 (1991).
23. A.V. Iogansen. Theor. Experim. Khim. **7**, 302 (1971).
24. L.D. Field, T.W. Hambley, and B.C.K. Yau. Inorg. Chem. **33**, 2009, (1994).
25. S. Scheiner. Hydrogen bonding: a theoretical perspective. Oxford University Press, Oxford, N.Y. 1997.
26. H. Gunter. NMR spectroscopy. John Wiley & Sons, Chichester, N.Y. 1980.
27. (*a*) G. Orlova and S. Scheiner. J. Phys. Chem. A, **102**, 4813 (1998); (*b*) G. Orlova, S. Scheiner, and T. Kar. J. Phys. Chem. A, **103**, 514 (1999).
28. (*a*) M.G. Basallote, J. Duran, M.J. Fernandez-Trujillo, M.A. Manez, and J.R. Torre. J. Chem. Soc. Dalton Trans. 7445 (1998); (*b*) M. G.Basallote, J. Duran, M.J. Fernandez-Trujillo, and M.A. Manez. J. Chem. Soc. Dalton Trans. 2205 (1998).